THE JOURNAL OF PHYSICAL CHEMISTRY Letters

Letter

Cite This: J. Phys. Chem. Lett. 2018, 9, 4886−4892

pubs.acs.org/JPCL

Kinetic Schemes in Open Interacting Systems

Abraham Nitzan[†,‡] and Michael Galperin*[,¶]

[†]Department of Chemistry, University of Pennsylvania, Philadelphia, Pennsylvania 19104, United States

[‡]School of Chemistry, Tel Aviv University, Tel Aviv 69978, Israel

[¶]Department of Chemistry and Biochemistry, University of California at San Diego, La Jolla, California 92093, United States

ABSTRACT: We discuss utilization of kinetic schemes for description of open interacting systems, focusing on vibrational energy relaxation for an oscillator coupled to a nonequilibirum electronic bath. Standard kinetic equations with constant rate coefficients are obtained under the assumption of time scale separation between the system and bath, with the bath dynamics much faster than that of the system of interest. This assumption may break down in certain limits, and we show that ignoring this may lead to qualitatively wrong predictions. Connection with more general, nonequilibrium Green's function (NEGF) analysis is demonstrated. Our considerations are illustrated within generic molecular junction models with electron−vibration coupling.

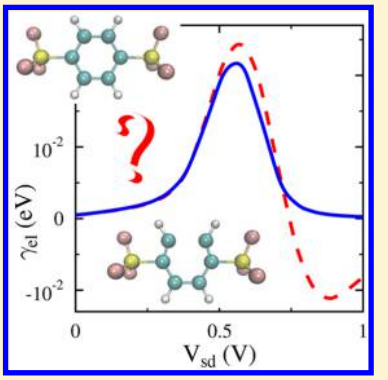

Development of experimental techniques on the nanoscale has made studies of single-molecule junctions possible. These experiments yield unique possibilities to explore physical and chemical properties of molecules by measuring their responses to external perturbations. Following experimental advances, there was rapid development of theoretical approaches. Today a variety of techniques, ranging from diagrammatic expansions (such as, e.g., the nonequilibrium Green function (NEGF),[1,2] quantum master equation,[3,4] and Hubbard NEGF[5,6]) to approximate treatments of strongly correlated systems (e.g., dynamical mean field theory[7] and beyond[8]) and to numerically exact methods (e.g., renormalization group techniques[9−12] and continuous time quantum Monte Carlo[13−15]), are available. Implementation of such schemes, particularly the numerically exact approaches, is often expensive, and their applications for simulations of realistic systems is limited.

At the same time, simple kinetic schemes have been widely and successfully utilized in the description of rate phenomena in open molecular systems (for example, donor−bridge−acceptor (DBA) molecular complexes).[16−23] Such schemes lead to a description of system states connected by rate processes whose Markov limit description provides "rate coefficients" that enter into the kinetic description (master equation) of the system evolution. Such Markov limit descriptions rely on time scale separation between the observed system evolution and dynamic processes that determine the rates; the latter usually involves the dynamics of relaxation in the bath. Obviously, the details of such kinetic schemes depend on the way system−bath separation is defined and used. The general practice dictated by balance between simplicity and rigor takes "the system" to be comprised by the observed variables together (when possible) with other variables whose inclusion makes the dynamics Markovian. This practice should be exercised with caution because even if conditions for time scale separations are established in a given range, they may become invalid in other domains of operation. Such situations are well-known in classical dynamics. For example, transition state theory (TST) of molecular rate processes assumes that molecular degrees of freedom except the reaction coordinate are at thermal equilibrium (and therefore can be taken to be part of the thermal environment). TST breaks down when the observed rate is on the order of, or faster than, the rate of thermal relaxation in the molecule, as demonstrated in the Kramers theory of activated rate processes.[24]

Importantly, even if the assumed time scale separation holds near equilibrium, it might fail far from it. The reason is that systems interacting with their equilibrium surrounding remain within the energetic domain of thermal energy, while systems coupled to nonequilibrium environments, e.g., under optical illumination or voltage bias, may be driven to energy domains where time scale separation does not hold. Thus, while situations of the first kind (such as activated barrier crossing) are well understood and documented, mathematically equivalent circumstances in nonequilibrium systems have been often overlooked. One such case is the vibrational dynamics of molecules adsorbed at or bridging between metallic interfaces due to coupling to the thermal electronic baths. Molecular vibrational motion is sensitive to the electronic occupation of the molecule, which in turn is affected by the molecule and metal electronic structure, their mutual coupling, and the junction voltage bias. A common approximation, equivalent to the fast bath assumption discussed above, is to disregard the

Received: June 15, 2018
Accepted: August 10, 2018
Published: August 10, 2018

DOI: 10.1021/acs.jpclett.8b01886
J. Phys. Chem. Lett. 2018, 9, 4886−4892

effect of vibrational dynamics on the electronic subsystem, representing the latter by a thermal electronic bath or, for a biased (current carrying) junction, by the corresponding steady-state electronic distribution, assumed unaffected by the vibrational process. This level of description, which effectively takes the molecular electronic degrees of freedom as part of the (generally nonequilibrium) electronic bath,[25−27] has been recently used to discuss bias-induced vibrational instabilities.[28−30] While the limitations of such treatments are sometimes pointed out,[30] in other publications, they are ignored. Indeed, such instabilities were recently claimed[31] to be generic properties of wires whose conduction is dominated by distinct electronic resonances (or, in the language of ref 31, by "separated" electronic states).

It should be noted that, in general, zero-order treatments of the kind described above are known to violate conservation laws.[32,33] Thus, notwithstanding their usefulness in many applications, such treatment should be regarded with caution, in particular, when unusual behaviors are observed. For example, the observation of a negative sign of the vibrational dissipation rate at an apparent steady state of a molecular junction should not be regarded as an indicator of a true vibrational instability in the system but (like in linear stability analysis of nonlinear differential equations) as an indication of failure of the underlying assumptions that lead to such a result. It should be emphasized that (again, as in linear stability analysis) such analysis can be useful as an indicator that a real stable state exists elsewhere (which in a real anharmonic molecule may or may not lie beyond a bond-breaking threshold). Still, many low-order treatments[28,29] of vibrational instabilities in harmonic bridge models of molecular junctions leave the reader with the message that the observed "runaway phonon" describes the full physical behavior.

Exact numerical solutions[43] are obviously capable of exploring the correct physical picture. Here we show that an approximate self-consistent treatment that does not violate conservation laws can already avoid the qualitative pitfalls of a linear theory. We consider simple junction models with electron−vibration coupling (see Figure 1), treated within the NEGF theory. In this framework, the consequence of interaction between a system of interest (here the vibrational mode) and its environment (here the electronic subsystem) enters through self-energy terms that (a) directly describe relaxation and driving of the system of interest by its environment and (b) modify the Green functions that enter into the definition of these self-energies. A full calculation must therefore be self-consistent and take into account the mutual influence between the system and environment, namely, the effect of the environment on the system as well as the back-action from the system on the environment. We show that the basis of the zero-order approximation, the assumption of time scale separation between molecular electronic and vibrational degrees of freedom (i.e., ability to neglect back-action of molecular vibration on the electronic bath), does not hold automatically and in fact has a limited range of validity. Consequently, while regimes of significantly enhanced vibrational heating can be found in biased junctions with electron−phonon coupling (and heating transient spikes may occur following sudden parameter change), instabilities identified as the appearance of a negative vibrational dissipation rate do not occur. In our consideration below, the molecular vibration (system) is weakly coupled to the electronic degrees of freedom (bath), which is the usual setup in considerations of system and bath separation. We stress that even in this favorable situation kinetic considerations may lead to qualitative failures.

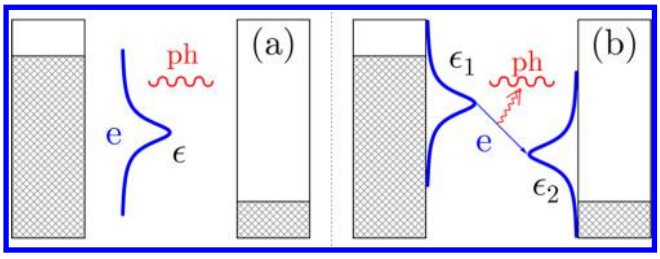

Figure 1. Molecular junction with electron−phonon interaction. Shown are models for a (a) single-level junction with polaronic coupling and (b) two-level junction with nonadiabatic coupling. Note that setup (b) favors phonon heating, which is maximized when the level spacing $\epsilon_1-\epsilon_2$ is close to the vibrational frequency.

Below, after introducing the model, we discuss its general treatment using NEGF and its connection to simple kinetic considerations. We consider the steady state of such a model under voltage bias and illustrate failures of standard kinetic description within numerical examples.

Model and Method. We consider a junction consisting of a molecular bridge M coupled to two contacts, L and R (Figure 1). Besides electronic degrees of freedom, a molecular vibration, modeled as a harmonic oscillator of frequency ω_0 coupled to the molecular electronic subsystem, is included. The contacts are reservoirs of free charge carriers, each at its own equilibrium. The model Hamiltonian is

$$\hat{H} = \hat{H}_M + \sum_{K=L,R} (\hat{H}_K + \hat{V}_{KM}) \tag{1}$$

$$\hat{H}_M = \sum_{m_1,m_2\in M} H^M_{m_1m_2}\hat{d}^\dagger_{m_1}\hat{d}_{m_2} + \omega_0\hat{a}^\dagger\hat{a} + \sum_{m_1,m_2\in M} U_{m_1m_2}(\hat{a}+\hat{a}^\dagger)\hat{d}^\dagger_{m_1}\hat{d}_{m_2} \tag{2}$$

$$\hat{H}_K = \sum_{k\in K} \epsilon_k \hat{c}^\dagger_k\hat{c}_k \tag{3}$$

$$\hat{V}_{KM} = \sum_{k\in K}\sum_{m\in M} (V_{km}\hat{c}^\dagger_k\hat{d}_m + \text{H.c.}) \tag{4}$$

where $\hat{d}^\dagger_m$ ($\hat{d}_m$) and $\hat{c}^\dagger_k$ ($\hat{c}_k$) create (annihilate) an electron in level m of the bridge and state k of contacts, respectively. $\hat{a}^\dagger$ ($\hat{a}$) creates (annihilates) vibrational quanta. V_{km} is a molecule−contact transfer matrix element, and $U_{m_1m_2}$ is the electron−phonon coupling strength. Below we consider two special cases of this Hamiltonian: a single bridge level with polaronic coupling to the vibrational mode, whereupon the last term in eq 2 takes the form $U(\hat{a}+\hat{a}^\dagger)\hat{d}^\dagger\hat{d}$ (Figure 1a) and a bridge comprising two coupled electronic levels, each coupled to its respective lead, with electron−vibration coupling of the form $U(\hat{a}+\hat{a}^\dagger)(\hat{d}^\dagger_2\hat{d}_1 + \hat{d}^\dagger_1\hat{d}_2)$.

We treat the electron−vibration coupling, last term in eq 2, within the standard diagrammatic technique. According to the rules for building conserving approximations,[32,33] one starts from the Luttinger−Ward functional,[2,34] whose functional derivatives with respect to the electron and phonon (vibration) Green functions yield the electron self-energy due to coupling

DOI: 10.1021/acs.jpclett.8b01886
J. Phys. Chem. Lett. 2018, 9, 4886−4892

to vibrations, $\Sigma^{(ph)}$, and the phonon self-energy due to coupling to electronic degrees of freedom, $\Pi^{(el)}$, respectively. For our discussion, it is important to stress that the electron and phonon Green functions in the functional are full (dressed) functions, with back-action of electrons on vibration and vice versa taken into account. Explicit expressions at second order of the diagrammatic technique in the electron−phonon interaction are[35,36]

$$\Sigma^{(ph)}_{m_1m_2}(\tau_1, \tau_2) = iD(\tau_1, \tau_2)\mathrm{Tr}[\mathbf{UG}(\tau_1, \tau_2)\mathbf{U}] \quad (5)$$

$$\Pi^{(el)}(\tau_1, \tau_2) = -i\mathrm{Tr}[\mathbf{UG}(\tau_1, \tau_2)\mathbf{UG}(\tau_2, \tau_1)] \quad (6)$$

where the Tr[···] is over electronic degrees of freedom in M and

$$G_{m_1m_2}(\tau_1, \tau_2) = -i\langle T_c \hat{d}_{m_1}(\tau_1)\hat{d}^{\dagger}_{m_2}(\tau_2)\rangle \quad (7)$$

$$D(\tau_1, \tau_2) = -i\langle T_c \hat{a}(\tau_1)\hat{a}^{\dagger}(\tau_2)\rangle \quad (8)$$

are the electron and phonon (vibration) Green functions (here T_c is the Keldysh contour ordering operator and $\tau_{1,2}$ are the contour variables). Below (for simplicity and to compare with previous studies) we will consider the quasiparticle limit for the phonon Green function.[37] Solving together the coupled eqs 5 and 6 constitutes the self-consistent Born approximation (SCBA). (Note that within SCBA the electron self-energy contains also the Hartree term, which comes from an additional contribution to the Luttinger−Ward functional and is responsible for shift of electronic levels due to the interaction. For relatively weak electron−vibration coupling, the shift is small and can be disregarded.) Dynamical characteristics are obtained by projecting these Keldysh functions onto real time. Lesser and greater projections of the self-energies eqs 5 and 6 describe respectively in- and out-fluxes into the corresponding degree of freedom due to its coupling to the other degrees of freedom in the system, while the retarded projection describes dissipation induced by the interaction. These projections are related by

$$\Pi^{(el)>}(t_1, t_2) - \Pi^{(el)<}(t_1, t_2) = \Pi^{(el)r}(t_1, t_2) - \Pi^{(el)a}(t_1, t_2) \quad (9)$$

where $\Pi^{(el)\,a}(t_1,t_2) = [\Pi^{(el)\,r}(t_2,t_1)]^*$ is the advanced projection and $t_{1,2}$ are physical times corresponding to the contour variables $\tau_{1,2}$. A similar relation holds for the electron self-energies obtained as projections of eq 5 onto the physical time.

At steady state, when correlation functions depend on time differences, one can Fourier transform eq 9. The right side of the expression is identified to be the vibrational dissipation rate due to coupling to electronic degrees of freedom

$$\gamma_{el}(\omega) = i(\Pi^{(el)>}(\omega) - \Pi^{(el)<}(\omega)) \quad (10)$$

which at the quasiparticle limit should be taken at $\omega = \omega_0$. The energy flux between the electronic and vibrational subsystems can be expressed by either of the two fluxes[38,39]

$$I^{(el)}_{ph} = -\int_0^{\infty} \frac{d\omega}{2\pi} (\Pi^{(el)<}(\omega)D^{>}(\omega) - \Pi^{(el)>}(\omega)D^{<}(\omega)) \quad (11)$$

$$I^{(ph)}_{el} = \int \frac{dE}{2\pi}\mathrm{Tr}[\Sigma^{(ph)<}(E)\mathbf{G}^{>}(E) - \Sigma^{(ph)>}(E)\mathbf{G}^{<}(E)] \quad (12)$$

which can be shown by substituting for the self-energies Σ and Π the corresponding projections of eqs 5 and 6, respectively, to be equal in magnitude and opposite in sign. These fluxes are caused by the electron−phonon interaction. Equation 11 expresses the energy flux (in terms of vibrational quanta) into the vibrational system, while eq 12 expresses the flux for population redistribution between energy levels of the electronic subsystem. Because of the charge-conserving character of the electron−phonon interaction, this flux vanishes, which at the quasi-particle limit leads to[40]

$$N_{\omega_0} = i\Pi^{(el)<}(\omega_0)/\gamma_{el}(\omega_0) \quad (13)$$

Here, $N_{\omega_0} = \langle \hat{a}^{\dagger}\hat{a}\rangle$ is the nonequilibrium average phonon population.

As discussed above, zero-order treatments that lead to standard kinetic schemes for this problem assume time scale separation between electronic and vibrational equilibration times (usually treating the vibrational subsystem as much slower than its electronic counterpart), thus disregarding back-action of the phonon on the electronic subsystem. Mathematically, this is manifested by disregarding the contribution to the electron self-energy due to coupling to vibration, eq 5, and employing the resulting zero-order electronic Green functions in evaluation of phonon self-energy eq 6. While the argument of time scale separation seems reasonable, it may lead to erroneous predictions. We note in passing that within diagrammatic perturbation theory, substituting the full (dressed) Green function with the bare one in the Luttinger−Ward functional leads to violation of conservation laws in the system.[41] In the Markov limit, when self-energies simplify into transition rates, such substitution corresponds to a statement that rates are kept constant irrespective of the actual state of the system.

Below we illustrate some consequences of breakdown of such a time scale separation assumption with numerical examples for the model junctions shown in Figure 1. Model (a) comprises a single molecular electronic level coupled to the two metal electrodes and to a single vibration, with $H^M_{mm} \to \epsilon$ and $U_{mm} \to U$. Model (b) involves two molecular levels and one vibrational mode with $H^M_{m_1m_2} = \delta_{m_1,m_2}\epsilon_{m1} - (1 - \delta_{m_1,m_2})t$, $U_{m_1m_2} = (1 - \delta_{m_1,m_2})U$, and V_{km} is V_{k1} when $k \in L$ and V_{k2} when $k \in R$.

Numerical Results. We start with model (a), a single electronic level coupled to a molecular vibration (Figure 1a). Electron escape rates to contacts are taken as $\Gamma_L = \Gamma_R = 0.1$ eV. The frequency of the molecular vibration is set to $\omega_0 = 0.1$ eV, and for the electron−vibration coupling, we take $U = 0.05$ eV. The contact temperature is taken as $T = 300$ K. The Fermi energy is chosen as the energy origin $E_F = 0$. We apply a bias $V_{sd} = 3$ V across the junction symmetrically ($\mu_L = 1.5$ eV and $\mu_R = -1.5$ eV) and consider the steady state of the system when level ϵ is moved in and out of the bias window. Calculations are performed on energy grid spanning the range from −4 to 4 eV with step 10^{-4} eV. We compare the results of zero-order simulation, where the rate (eq 10) and population (eq 13) are obtained utilizing the zero-order electron Green function in eq 6, with SCBA results, where the self-consistent procedure takes into account the mutual influence of electron and vibrational degrees of freedom in the system. In the latter case, convergence is assumed to be reached when the

DOI: 10.1021/acs.jpclett.8b01886
J. Phys. Chem. Lett. 2018, 9, 4886−4892

difference in values of the electron density matrix at subsequent steps is less than 10^{-12}.

Figure 2a shows phonon dissipation rates as a function of gate voltage. As expected, the rate is maximum when level ϵ

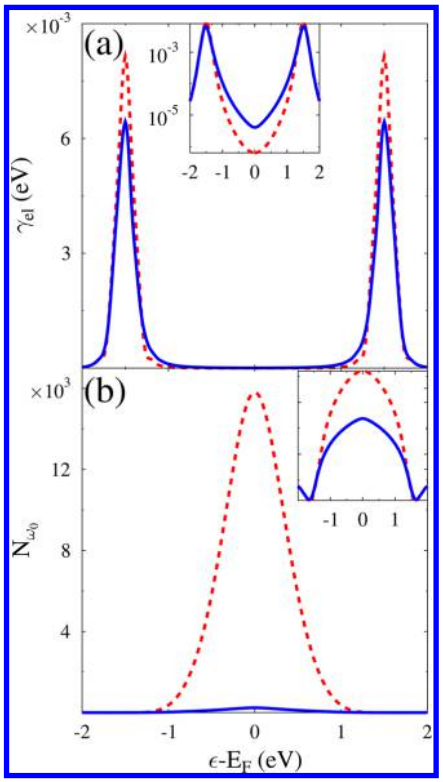

Figure 2. Steady-state simulation of the single-level model (Figure 1a) within the SCBA (solid line, blue) and Born approximation (dashed line, red) schemes at V_{sd} = 3 V. Shown are (a) the phonon dissipation rate due to coupling to electrons, eq 10, and (b) the nonequilibrium phonon population, eq 13, vs position of the level ϵ. Insets are logarithmic scale plots of the main panels.

crosses the lead chemical potential where the possibility of effective creation of electron−hole pairs exceeds that of destruction, which leads to strong dissipation of vibrational energy; the rate is much lower away from chemical potentials where both creation and destruction of electron−hole pairs have similar probability. Qualitatively, both schemes give the same behavior. However, self-consistency of the SCBA allows one to account for multiple phonon scatterings, which results in a significantly higher dissipation rate for the vibration within the bias window. As a result, the standard kinetic scheme significantly overestimates heating of molecular vibration by electron flux, as demonstrated in Figure 2b. This results in underestimation of stability of the molecular junction when analyzed within the kinetic scheme.

Discrepancy between SCBA and the standard kinetic scheme is even more pronounced for nonadiabatic electron−phonon coupling (model b). This is the two-level model (Figure 1b) used in refs 28, 29, and 31 to demonstrate bias-induced vibrational instabilities. As above, we consider a stable steady state and its characteristics rate (eq 10) and population (eq 13). We note that phonon back-action on the electron degrees of freedom, characterized by the self-energy (eq 5), is proportional to population N_{ω_0}. That is, within the harmonic oscillator model, any electron pumping can be compensated by phonon back-action when a large enough N_{ω_0} is reached. Thus, one expects that a stable steady state will be always achievable and no phonon runaway will be observed. Taking into account that molecular vibrations are not harmonic at high excitations, the reasonable question to ask is if N_{ω_0} compensating for electronic pumping is big enough to actually break the molecular bond. We note that SCBA analysis of the model was performed in the literature previously.[35,42] Our goal here is comparison between the SCBA and kinetic scheme predictions.

The electronic levels are chosen at equilibrium as $\epsilon_1 = -0.15$ eV and $\epsilon_2 = 0.55$ eV. Following ref 28, we assume that the two electronic levels are pinned to their respective baths, so that positions of the levels are shifted with bias together with corresponding chemical potentials. Electron escape rates to contacts are $\Gamma_L = 0.3$ eV and $\Gamma_R = 0.1$ eV. The other parameters are as those in Figure 2.

Figure 3 compares zero-order and SCBA results for the phonon dissipation rate γ_{el}, eq 10. In agreement with previous considerations,[28,29,31] the zero-order calculation predicts instability for the resonance condition, showing runaway heating of the vibration when the electron hopping matrix element t is small (see the lower right corner of the dissipation rate map shown in Figure 3a). The corresponding SCBA results are shown in Figure 3b: no instability (negative dissipation rate) is observed in this case. To make the comparison easier, Figure 3c shows horizontal cuts of the two maps for t = 0.05 eV. The inset in this panel shows the nonequilibrium population of the mode at this time. While the zero-order simulation predicts negative damping (and hence instability), the SCBA result indicates finite heating of the mode with bias. Note that the population at V_{sd} = 1 V is about $N_{\omega_0} = 20$, which for $\omega_0 = 0.1$ eV gives a total vibrational energy of 2 eV (190 kJ/mol), insufficient for breaking most molecular bonds.

The qualitative nature of this results, that is, the absence of true instability in the models considered, does not depend on the parameters used in the calculation. We note that phonon back-action on the electron degrees of freedom, characterized by the self-energy (eq 5), is proportional to population N_{ω_0}. That is, within the harmonic oscillator model, any electron pumping can be compensated by phonon back-action when a large enough N_{ω_0} is reached. Thus, one expects that a stable steady state will be always achievable and no phonon runaway will be observed. Depending on the actual molecular force field, the corresponding compensation for electronic pumping may be quite large[43] and, depending on the molecule, may be beyond the bond-breaking threshold of the real anharmonic molecule. Such bond-breaking should not however be deduced just from the prediction of the negative vibrational dissipation rate obtained from the standard kinetic analysis. Note that negativity of the vibrational dissipation rate in a steady-state situation is an indication of qualitative failure of the zero-order treatment.

Figure 4 shows the electronic energy distribution in levels (a) ϵ_1 and (b) ϵ_2 calculated with (solid line, SCBA) and without (dashed line, zero-order) vibrational back-action taken into account. In this calculation, we used t = 0.05 eV and V_{sd} = 0.9 V. These parameters correspond to the most unstable (most negative dissipation rate) prediction of the Born (zero-order) calculation (Figure 3c). One sees that electron−

DOI: 10.1021/acs.jpclett.8b01886
J. Phys. Chem. Lett. 2018, 9, 4886−4892

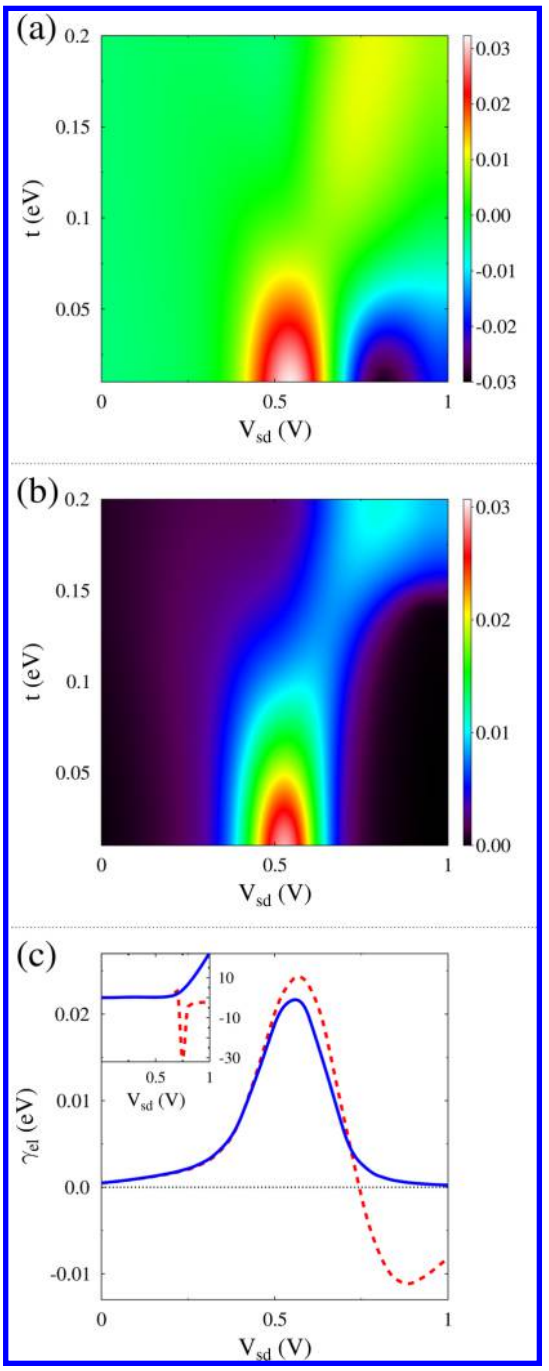

Figure 3. Steady-state simulation of the two-level model (Figure 1b). Shown is a map of the phonon dissipation rate, eq 10, vs the applied bias, V_{sd}, and electron hopping, t, for (a) zero-order and (b) SCBA simulations. (c) Results of the two simulations at $t = 0.05$ eV. The red dotted line presents kinetic scheme results, and the solid blue line represents SCBA results. The inset shows the average vibrational population N_{ω_0}, eq 13, as a function of V_{sd}.

vibration coupling promotes redistribution of electron population between levels ϵ_1 and ϵ_2; the effect is significant even for $U \ll \Gamma_{L,R}$. We note in passing that the effect of the coupling on electronic coherence (not shown) is even more drastic.

Standard rate theories that are very useful in the analysis of many chemical dynamics phenomena usually rely on time scale separation between the system of interest and its environment. Failure of such separation in treatments of systems interacting

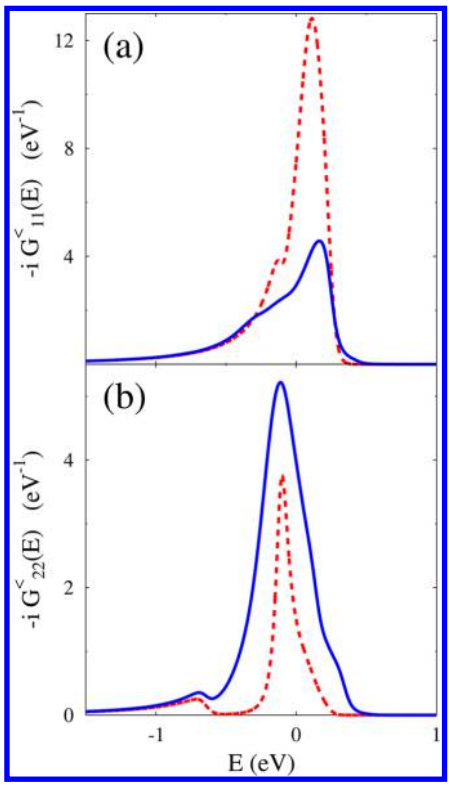

Figure 4. Steady-state simulation of the two-level model (Figure 1b). Shown are electron population distributions for levels (a) ϵ_1 and (b) ϵ_2. Kinetic scheme results (dashed line, red) are compared with the SCBA (solid line, blue) simulations.

with equilibrium environments is usually handled by redefining the boundaries between the system and bath. Extra care is needed when the system is driven by a nonequilibrium environment, where the driving may move the system into regimes where time scale separation does not hold. We have discussed the implications of the common time scale separation assumption used in analyzing the time evolution vibrational energy in biased molecular junctions. Using such treatments outside of their range of validity can lead to qualitatively wrong predictions. As an example, we considered generic models of molecular junctions with electron−phonon interaction treated within the NEGF-SCBA level of theory. A standard time scale separation argument suggests that phonon back-action on electronic degrees of freedom can be disregarded. Such an approximation, however, formally violates conservation laws and can fail both qualitatively and quantitatively when inadvertently carried into regimes where time scale separation does not hold. Not accounting for this back-action leads to an overestimated heating of molecular vibrations in the standard single electronic level model of current carrying molecular junctions as compared with the renormalized (SCBA) treatment (Figure 1a). This discrepancy with the SCBA is even more pronounced for the nonadiabatic electron−phonon coupling model (Figure 1b). Analysis of this model within the time scale separation assumption has indicated the existence of bias-induced vibrational instability in molecular junctions, which was associated with appearance of a negative vibrational dissipation rate. However, a self-consistent calculation, here carried at the NEGF-SCBA level, shows that a stable steady state is reached for any set of parameters (any electronic heating rate).

DOI: 10.1021/acs.jpclett.8b01886
J. Phys. Chem. Lett. 2018, 9, 4886−4892

Depending on the molecular force field, the molecule−metal coupling, and the potential bias, the molecular energy at steady state obtained in such a (harmonic model) calculation, which can be high,[43] may or may not exceed the actual bond-breaking threshold of the real anahrmonic molecule. We note that sudden changes in the electronic system (such as fast switch-on of bias) can lead to transient heating spikes that, for a harmonic oscillator, will eventually relax to the new steady state but in real molecules can lead to bond breaking even if the steady-state population is below the breaking threshold. For slow switch-on of the bias, observation of vibrational instabilities in calculations done under the standard system−bath time scale separation assumption should be taken as indications that this assumption fails and that higher-level studies are needed to reach conclusions about actual bond breaking.

Rate theories using standard kinetic schemes are often a method of choice that has been repeatedly reliable and useful for modeling chemical dynamics. Extra caution should be exercised when employing such methods in nonequilibrium systems because they usually disregard back-action of the system onto its bath(s), which, as we showed, may lead to erroneous predictions. Development of advanced kinetic schemes for the latter systems is a goal of future research.

AUTHOR INFORMATION

Corresponding Author

*E-mail: migalperin@ucsd.edu. Phone: +1-858-246-0511.

ORCID

Abraham Nitzan: 0000-0002-8431-0967

Michael Galperin: 0000-0002-1401-5970

Notes

The authors declare no competing financial interest.

ACKNOWLEDGMENTS

A.N. is supported by the National Science Foundation (Grant No. CHE-1665291), the Israel Science Foundation, the US−Israel Binational Science Foundation, and the University of Pennsylvania. M.G. is supported by the National Science Foundation under CHE-1565939 and by the Department of Energy under DE-SC0018201.

REFERENCES

(1) Haug, H.; Jauho, A.-P. *Quantum Kinetics in Transport and Optics of Semiconductors*; Springer: Berlin, Heidelberg, 2008.

(2) Stefanucci, G.; van Leeuwen, R. *Nonequilibrium Many-Body Theory of Quantum Systems. A Modern Introduction*; Cambridge University Press: New York, 2013.

(3) Leijnse, M.; Wegewijs, M. R. Kinetic Equations for Transport through Single-Molecule Transistors. *Phys. Rev. B: Condens. Matter Mater. Phys.* **2008**, *78*, 235424.

(4) Kern, J.; Grifoni, M. Transport across an Anderson Quantum Dot in the Intermediate Coupling Regime. *Eur. Phys. J. B* **2013**, *86*, 384.

(5) Chen, F.; Ochoa, M. A.; Galperin, M. Nonequilibrium Diagrammatic Technique for Hubbard Green functions. *J. Chem. Phys.* **2017**, *146*, 092301.

(6) Miwa, K.; Chen, F.; Galperin, M. Towards Noise Simulation in Interacting Nonequilibrium Systems Strongly Coupled to Baths. *Sci. Rep.* **2017**, *7*, 9735.

(7) Aoki, H.; Tsuji, N.; Eckstein, M.; Kollar, M.; Oka, T.; Werner, P. Nonequilibrium Dynamical Mean-Field Theory and Its Applications. *Rev. Mod. Phys.* **2014**, *86*, 779−837.

(8) Rohringer, G.; Hafermann, H.; Toschi, A.; Katanin, A. A.; Antipov, A. E.; Katsnelson, M. I.; Lichtenstein, A. I.; Rubtsov, A. N.; Held, K. Diagrammatic Routes to Nonlocal Correlations Beyond Dynamical Mean Field Theory. *Rev. Mod. Phys.* **2018**, *90*, 025003.

(9) Paaske, J.; Rosch, A.; Wölfle, P. Nonequilibrium Transport through a Kondo Dot in a Magnetic Field: Perturbation Theory. *Phys. Rev. B: Condens. Matter Mater. Phys.* **2004**, *69*, 155330.

(10) Anders, F. B. Steady-State Currents through Nanodevices: A Scattering-States Numerical Renormalization-Group Approach to Open Quantum Systems. *Phys. Rev. Lett.* **2008**, *101*, 066804.

(11) Kirino, S.; Fujii, T.; Zhao, J.; Ueda, K. Time-Dependent DMRG Study on Quantum Dot under a Finite Bias Voltage. *J. Phys. Soc. Jpn.* **2008**, *77*, 084704.

(12) Laakso, M. A.; Kennes, D. M.; Jakobs, S. G.; Meden, V. Functional Renormalization Group Study of the Anderson-Holstein Model. *New J. Phys.* **2014**, *16*, 023007.

(13) Cohen, G.; Gull, E.; Reichman, D. R.; Millis, A. J. Green's Functions from Real-Time Bold-Line Monte Carlo Calculations: Spectral Properties of the Nonequilibrium Anderson Impurity Model. *Phys. Rev. Lett.* **2014**, *112*, 146802.

(14) Cohen, G.; Gull, E.; Reichman, D. R.; Millis, A. J. Taming the Dynamical Sign Problem in Real-Time Evolution of Quantum Many-Body Problems. *Phys. Rev. Lett.* **2015**, *115*, 266802.

(15) Ridley, M.; Singh, V. N.; Gull, E.; Cohen, G. Numerically Exact Full Counting Statistics of the Nonequilibrium Anderson Impurity Model. *Phys. Rev. B: Condens. Matter Mater. Phys.* **2018**, *97*, 115109.

(16) Migliore, A.; Nitzan, A. Nonlinear Charge Transport in Redox Molecular Junctions: A Marcus Perspective. *ACS Nano* **2011**, *5*, 6669−6685.

(17) Einax, M.; Dierl, M.; Nitzan, A. Heterojunction Organic Photovoltaic Cells as Molecular Heat Engines: A Simple Model for the Performance Analysis. *J. Phys. Chem. C* **2011**, *115*, 21396−21401.

(18) Migliore, A.; Nitzan, A. Irreversibility and Hysteresis in Redox Molecular Conduction Junctions. *J. Am. Chem. Soc.* **2013**, *135*, 9420−9432.

(19) Einax, M.; Nitzan, A. Network Analysis of Photovoltaic Energy Conversion. *J. Phys. Chem. C* **2014**, *118*, 27226−27234.

(20) Craven, G. T.; Nitzan, A. Electron Transfer across a Thermal Gradient. *Proc. Natl. Acad. Sci. U. S. A.* **2016**, *113*, 9421−9429.

(21) Craven, G. T.; Nitzan, A. Electron Transfer at Thermally Heterogeneous Molecule-Metal Interfaces. *J. Chem. Phys.* **2017**, *146*, 092305.

(22) Chen, R.; Craven, G. T.; Nitzan, A. Electron-Transfer-Induced and Phononic Heat Transport in Molecular Environments. *J. Chem. Phys.* **2017**, *147*, 124101.

(23) Craven, G. T.; Nitzan, A. Electrothermal Transistor Effect and Cyclic Electronic Currents in Multithermal Charge Transfer Networks. *Phys. Rev. Lett.* **2017**, *118*, 207201.

(24) Kramers, H. A. Brownian Motion in a Field of Force and the Diffusion Model of Chemical Reactions. *Physica* **1940**, *7*, 284−304.

(25) Agarwalla, B. K.; Jiang, J.-H.; Segal, D. Full Counting Statistics of Vibrationally Assisted Electronic Conduction: Transport and Fluctuations of Thermoelectric Efficiency. *Phys. Rev. B: Condens. Matter Mater. Phys.* **2015**, *92*, 245418.

(26) Strasberg, P.; Schaller, G.; Schmidt, T. L.; Esposito, M. Fermionic Reaction Coordinates and Their Application to an Autonomous Maxwell Demon in the Strong-Coupling Regime. *Phys. Rev. B: Condens. Matter Mater. Phys.* **2018**, *97*, 205405.

(27) Dou, W.; Subotnik, J. E. Universality of Electronic Friction. II. Equivalence of the Quantum-Classical Liouville Equation Approach with von Oppen's Nonequilibrium Green's Function Methods out of Equilibrium. *Phys. Rev. B: Condens. Matter Mater. Phys.* **2018**, *97*, 064303.

(28) Lü, J.-T.; Hedegård, P.; Brandbyge, M. Laserlike Vibrational Instability in Rectifying Molecular Conductors. *Phys. Rev. Lett.* **2011**, *107*, 046801.

(29) Simine, L.; Segal, D. Vibrational Cooling, Heating, and Instability in Molecular Conducting Junctions: Full Counting Statistics Analysis. *Phys. Chem. Chem. Phys.* **2012**, *14*, 13820−13834.

DOI: 10.1021/acs.jpclett.8b01886
J. Phys. Chem. Lett. 2018, 9, 4886−4892

(30) Gelbwaser-Klimovsky, D.; Aspuru-Guzik, A.; Thoss, M.; Peskin, U. High Voltage Assisted Mechanical Stabilization of Single-Molecule Junctions. *Nano Lett.* **2018**, *18*, 4727−4733.
(31) Foti, G.; Vázquez, H. Origin of Vibrational Instabilities in Molecular Wires with Separated Electronic States. *J. Phys. Chem. Lett.* **2018**, *9*, 2791−2796.
(32) Baym, G.; Kadanoff, L. P. Conservation Laws and Correlation Functions. *Phys. Rev.* **1961**, *124*, 287−299.
(33) Baym, G. Self-Consistent Approximations in Many-Body Systems. *Phys. Rev.* **1962**, *127*, 1391−1401.
(34) Luttinger, J. M.; Ward, J. C. Ground-State Energy of a Many-Fermion System. II. *Phys. Rev.* **1960**, *118*, 1417−1427.
(35) Park, T.-H.; Galperin, M. Self-Consistent Full Counting Statistics of Inelastic Transport. *Phys. Rev. B: Condens. Matter Mater. Phys.* **2011**, *84*, 205450.
(36) Gao, Y.; Galperin, M. Optical Spectroscopy of Molecular Junctions: Nonequilibrium Green's Functions Perspective. *J. Chem. Phys.* **2016**, *144*, 174113.
(37) Mahan, G. D. *Many-Particle Physics*; Kluwer Academic/Plenum Publishers: New York, Boston, Dordrecht, London, Moscow, 1990.
(38) Galperin, M.; Nitzan, A.; Ratner, M. A. Heat Conduction in Molecular Transport Junctions. *Phys. Rev. B: Condens. Matter Mater. Phys.* **2007**, *75*, 155312.
(39) Datta, S. *Electronic Transport in Mescoscopic Systems*; Cambridge University Press: Cambrigde, U.K., 1995.
(40) Fransson, J.; Galperin, M. Spin Seebeck Coefficient of a Molecular Spin Pump. *Phys. Chem. Chem. Phys.* **2011**, *13*, 14350−14357.
(41) Kadanoff, L. P.; Baym, G. *Quantum Statistical Mechanics*; Frontiers in Physics; W. A. Benjamin, Inc.: New York, 1962.
(42) Ryndyk, D. A.; Hartung, M.; Cuniberti, G. Nonequilibrium Molecular Vibrons: An Approach Based on the Nonequilibrium Green Function Technique and the Self-Consistent Born Approximation. *Phys. Rev. B: Condens. Matter Mater. Phys.* **2006**, *73*, 045420.
(43) Schinabeck, C.; Härtle, R.; Thoss, M. Hierarchical Quantum Master Equation Approach to Electronic−Vibrational Coupling in Nonequilibrium Transport Through Nanosystems: Reservoir Formulation and Application to Vibrational Instabilities. *Phys. Rev. B: Condens. Matter Mater. Phys.* **2018**, DOI: 10.1103/PhysRevB.97.235429.

DOI: 10.1021/acs.jpclett.8b01886
J. Phys. Chem. Lett. 2018, 9, 4886−4892